SCIENCE CHINA
Physics, Mechanics & Astronomy

• Letter to the Editor •

December 2017 Vol. 60 No. 12: 124321
doi: 10.1007/s11433-017-9088-5

Characterization and modeling of wind-dominated ambient noise in South China Sea

DongGe Jiang[1,2], ZhengLin Li[1*], JiXing Qin[1], ZhaoHui Peng[1], and Hao Shao[1]

[1] *State Key Laboratory of Acoustics, Institute of Acoustics, Chinese Academy of Sciences, Beijing 100190, China;*
[2] *University of Chinese Academy of Sciences, Beijing 100190, China*

Received May 23, 2017; accepted August 7, 2017; published online October 24, 2017

Citation: D. G. Jiang, Z. L. Li, J. X. Qin, Z. H. Peng, and H. Shao, Characterization and modeling of wind-dominated ambient noise in South China Sea, Sci. China-Phys. Mech. Astron. **60**, 124321 (2017), doi: 10.1007/s11433-017-9088-5

The action of wind on the sea surface plays an important role in the noise generation mechanism. Sea surface wind speed can be estimated accurately provided there is an accurate understanding of the relationship between the ocean ambient noise and wind speed. Many measurements and analyses of the wind dependence of ambient noise have been conducted. The approximate empirical rule given by Wenz [1] states that in the frequency band between 0.5 and 5 kHz, the ambient sea-noise spectrum levels decrease 5 dB per octave with increasing frequency and increase 5 dB with each doubling of the wind speed from 2.5 to 40 knots (1 knots=1.853 km/h=0.515 m/s). Piggott [2] found that the noise spectrum level in the high-frequency band depends linearly on the logarithm of the surface wind speed in shallow water. Crouch and Burt [3] found a similar linear relationship in deep water. The seasonal variability of the wind dependence of ambient noise was identified by Klusek and Lisimenka [4] in the southern Baltic Sea due to changes in the hydrological environment. During their analysis of typhoon-generated noise in the South China Sea, Wang et al. [5] and Liu et al. [6] used the proportion coefficient 3 for the noise source intensity in the logarithm of the local wind speed to calculate the noise field. In the same Beaufort scale, Wen et al. [7] found a better correlation between the ocean ambient noise and wind speed during a typhoon than during non-typhoon periods in the South China Sea.

There are many effective analytical and numerical models [8] of ambient ocean noise based on full wave theory, ray theory, and parabolic approximation theory, and other modified models have been applied under different conditions [5,9]. A unit source level, defined as the source level per unit area of ocean surface, is used to produce noise levels and array responses. One source of wind-source level values is derived via an empirical model (Wislon [10]) based on the "white-cap index", but it applies only to frequencies between 50 and 1000 Hz and wind speeds from 10 to 30 knots. Another source of wind-source level values can be inferred from measured noise levels by the use of models to extract the propagation effects (Kuperman and Ferla [11], Kewley et al. [12]), but these measurements are conducted in shallow water only and the maximum allowable frequency is 3.2 kHz.

In this letter, we investigated the wind dependence of ambient sea noise based on data obtained from a noise measurement experiment conducted in the deep-water area of the South China Sea. We obtained the ambient noise spectra in the wind speed grouping based on the quantitative relationship between the wind speed and noise spectrum level. We established a ray model to forecast the noise spectra for different wind speeds. We revised the existing wind-source level formula by minimizing the sum of the deviation between the experimental noise spectra and the numerical results for the wind-dominated frequency band and wind speed grouping. The good agreement between the wind-dominated ambient noise spectrum from the revised model and the experimental data indicates the model's potential for use in predicting

*Corresponding author (email: lzhl@mail.ioa.ac.cn)

wind-dependent ambient noise levels in the South China Sea.

In 2015, we moored a submersible buoy system on the bottom in the deep-water area of the South China Sea. This system consisted of 20 distributed underwater signal recorders ranging from 120 to 1300 m in depth at different vertical intervals. The sample rate of the hydrophones was 16 kHz. We obtained the sound speed profile shown in Figure 1(a) from measurements taken by an underwater sound velocity meter during the experiment. The depth of the sound channel axis is about 1100 m and the sound speed at the bottom is 1493 m/s, which is less than that at sea surface, 1544 m/s. We used the data collected near the depth of the sound channel axis in our data processing.

The experimental site is typically shielded against the traffic noise of the major shipping lanes. The absence of human activities (such as shipping and pile driving) in the experimental site made it possible to record the wind-dominated ambient noise. The synchronous meteorological data for the experimental area, which was provided by the National Marine Environmental Forecasting Center, contains wind speed and rain rate data for the entire area at 6 h intervals throughout the experimental period. The experiment lasted 43 d and the passage of a typhoon was also recorded. The recorded wind speeds in the South China Sea during the passage of the typhoon are shown in Figure 1(b). We obtained the shipping density by the automatic identification system. To highlight the wind-dominated influence, we removed noise data generated by rain or other accidental sources from our data processing. As the reference value of local wind speed, we used the nearest measured wind speed to the experimental site, due to its good correlation with noise as reported by Cato and Tavener [13].

We averaged the noise spectra in the 1/3-octave bandwidth for data processing. We represent the narrow band spectrum level of the experimental noise as follows:

$$NL^{e}(f_0) = 10\log_{10}\left[\frac{2}{Nf_s}\frac{1}{nf_H - nf_L + 1}\sum_{i=nf_L}^{nf_H}|X_i|^2\right] - M_v, \quad (1)$$

where X_i is the fast Fourier transform spectrum of the noise stationary section $x(i)$ in the ith frequency bin, f_0 is the central frequency, and f_s is the sample rate, N is the length of the processed noise, nf_L and nf_H are the start and end frequency numbers of the frequency band, respectively, and M_v is the sensitivity of the hydrophones.

Figure 2 shows the noise spectrogram and synchronous wind speeds. The apparent high intensity change in the noise spectrogram indicates the effect of the typhoon on October 3. Continuous strong wind speeds occurred from October 12 to 20 and the noise spectrum level at 508 Hz changed along with wind speed (Figure 2(b)). Therefore, in the following analysis, we focus on frequency bands above 500 Hz. We observed an average wind speed of 5 m/s at the experiment site. After data selection, the obtained noise was generated by fully dispersed wind speeds (Figure 3(a)), which is useful for analyzing wind dependence from measured noise data.

Based on the experimental results reported by many authors [3-6], noise intensity vs. logarithmic wind speed can be expressed as a linear relationship,

$$NL^{e}(f_i) = 10 \cdot n(f_i)\log_{10}U + M(f_i), \quad (2)$$

where U is the wind speed (m/s) at a standard height of 10 m, NL^{e} is the experimental noise spectrum level (in dB re 1 μPa^2/Hz) in the 1/3-octave frequency band with a central frequency f_i, $n(f)$ is the wind speed dependence coefficient, and $M(f)$ is the frequency-dependent function.

The linear dependence of NL^{e} on $10\log_{10}U$ is suitable only for a certain range of wind speeds. Wind speeds exceeding saturation speed may create higher sound attenuation due to the presence of dense bubble clouds and persistent bubble layers created under the sea surface during intense wave

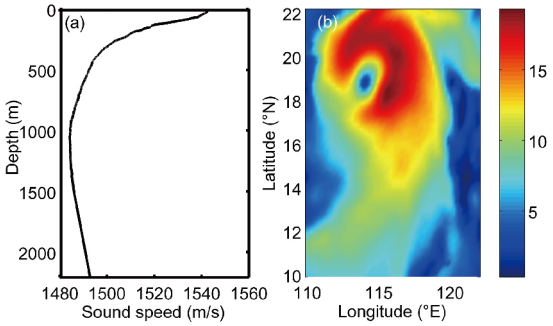

Figure 1 (Color online) (a) Sound speed profile recorded at the experimental site; (b) wind speeds in the South China Sea during the passage of a typhoon recorded by the synchronous meteorological data. The color bar values are the wind speeds (m/s).

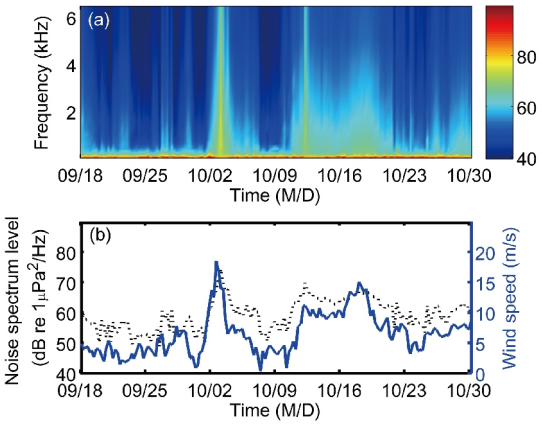

Figure 2 (Color online) Noise spectrogram and synchronous wind speeds. (a) Noise spectrogram for the period from September 18 to October 30, at frequencies from 20 to 6500 Hz. The color bar value indicates the noise spectrum level (in dB re 1 μPa^2 Hz^{-1}, re denotes the reference pressure in water is 1 μPa); (b) the solid line shows the synchronous wind speed and the dashed line shows the noise spectrum level at 508 Hz.

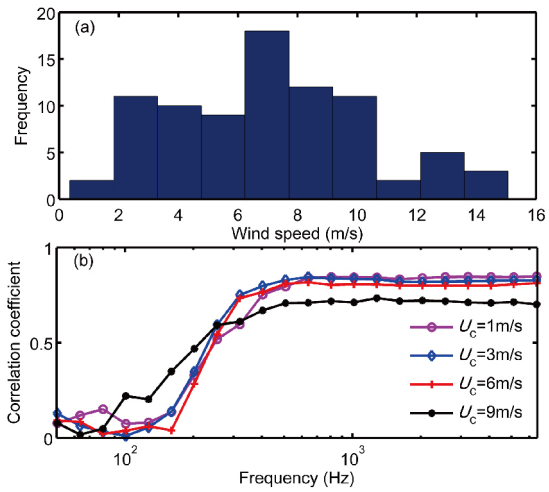

Figure 3 (Color online) (a) Wind speed frequency chart; (b) correlation coefficient between noise spectrum level and wind speeds for different U_c. The frequency band ranges from 500 to 6500 Hz.

breaking. Wind speeds less than the critical threshold may not create breaking waves so wind-generated noise may not dominate. In this letter, we did not consider saturation wind speed because the highest measured wind speed does not exceed the limit, as reported by Farmer and Lemon [14]. We selected the critical threshold wind speed (U_c) for our analysis.

Figure 3(a) shows the wind speed frequency chart after data selection in which the noise data generated by rain or other accidental sources was rejected. Suppose there are four different U_c values according to their positions in the wind speed frequency chart. Figure 3(b) shows the correlation coefficient between the noise spectrum level and wind speeds for different critical threshold wind speeds.

The noise spectrum level and wind speed have similar correlation coefficients when U_c=3 m/s and 6 m/s, and they have a higher correlation coefficient when U_c=1 m/s in the frequency range of 250-400 Hz. The reason for this difference is that low wind speeds cannot produce enough wind-generated noise energy to exert a significant wind-dependent influence in the low frequency band. U_c=9 m/s has a poor correlation coefficient due to a deficiency in the data because high wind speeds are rare except in extreme weather. We selected U_c=3 m/s due to its good correlation coefficient between the noise spectrum level and wind speed in the higher frequency range.

When the wind speed exceeds 3 m/s, we derived the noise-wind speed dependence coefficients and correlation coefficient using the least squares method. We observed a strong wind dependence (r≈0.8, where r is the correlation coefficient) in the frequency range of 0.5-6.4 kHz and an approximately quadratic noise-wind speed dependence ($n(f)$≈1.8) in the frequency range of 0.5-3.2 kHz, as shown in Table 1.

The noise spectrum levels in each wind speed grouping can be obtained based on the quantitative relationship between the wind speed and noise spectrum level at a wind-dominated frequency. When the frequency is fixed at 1016 Hz, the expression eq. (2) shows the linear relationship between the noise spectrum level and logarithmic wind speed. We selected temporal data whose spectrum level is the nearest to this line, and used its spectrum level as the noise spectrum level at certain wind speed. We chose six wind speeds from 4 to 14 m/s as our wind speed grouping. Then, we obtained the ambient noise spectrum levels in this wind speed grouping (dotted line in Figure 4).

By modeling the ambient noise, we can predict the noise field for different meteorological and hydrological conditions. In turn, if we know the real-time measured noise and one of the hydrological conditions and meteorological conditions, we can determine the other [15]. We developed a model based on the ray theory to predict the noise field. If we suppose a large number of noise sources (directionality $\sin\theta_s$) are distributed uniformly on an infinite sea surface in a

Table 1 Noise-wind speed dependence coefficients and correlation coefficient as a function of 1/3-octave frequency

Frequency (Hz)	$M(f)$	$n(f)$	r
508	47.0	1.7	0.83
640	45.6	1.8	0.84
806	45.0	1.8	0.84
1016	43.8	1.8	0.83
1280	43.0	1.8	0.82
1613	42.2	1.7	0.82
2032	40.9	1.7	0.82
2560	39.6	1.6	0.82
3225	38.4	1.6	0.82
4064	37.2	1.5	0.82
5120	36.2	1.4	0.83
6451	35.9	1.3	0.83

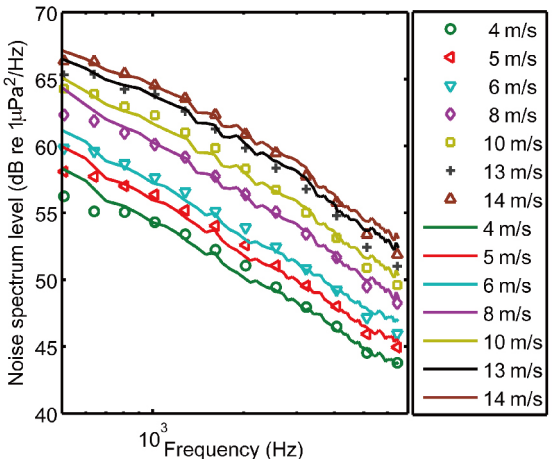

Figure 4 (Color online) Comparison of the experimental noise spectrum levels (dotted line) and noise spectrum levels forecasted by the revised model (solid line) when eq. (5) is adopted as the *SLW* for different wind speeds. The frequency band ranges from 500 to 7000 Hz.

range-independent environment, the noise level (NL^{c}) at the receiver can be expressed as follows [16]:

$$NL^{c} = SLW + 10\log_{10}\left(\left|2\pi\int_{0}^{\pi/2}\left[1 - R_{s}R_{b}e^{-as_{c}}\right]^{-1} \times\left(e^{-as_{p}} + R_{b}e^{-a(s_{c}-s_{p})}\right)\sin\theta_{s}\cos\theta_{r}d\theta_{r}\right|\right), \quad (3)$$

where SLW is the wind-source level (dB) and θ_{r} is the arrival angle at the receiver, R_{s} and R_{b} are surface and bottom power reflection coefficients at the surface and bottom grazing angles, respectively, and a is the volume absorption. s_{c} is the path length of a single ray cycle and s_{p} is the part-cycle path length (from receiver depth to the surface for one upward going ray). We used a two-layered bottom model to calculate NL^{c}. The thickness of sediment is 20 m. The density, sound speed, and attenuation with respect to the sediment layer are 1.6 g/cm^{3}, 1555 m/s, and $0.517\times f^{1.07}$ dB/λ (f is in unit of kHz), respectively, and the density, sound speed, and attenuation with respect to the half-infinite bottom are 1.8 g/cm^{3}, 1650 m/s, and $0.517\times f^{1.07}$ dB/λ (f is in unit of kHz) [17], respectively.

The wind-source level provided by Harrison [18] is not suitable for deep-water experimental data. Since the relationship between the noise spectra and frequency can be determined, we selected as revised parameters only the constant and wind-dependent coefficients in the SLW formula. We used a cost formula (eq. (4)) to determine the optimal parameters. The sum of the deviation between the experimental NL^{c} and numerical NL^{e} will reach a minimum if we search in a reasonable range to obtain the optimal constant and wind-dependent coefficients.

$$\text{Cost} = \min\sum_{f}\sum_{U}|NL^{c}(f,U) - NL^{e}(f,U)|, \quad (4)$$

where f is the 1/3-octave frequency (Hz) from 508 to 6451 Hz and U is wind speed (m/s) in the wind speed grouping shown in Figure 4.

According to the different $n(f)$ values shown in Table 1, SLW is expressed in two frequency bands. We have revised the wind-source level as follows:

$$SLW = \begin{cases} 58 - 6\cdot\log_{10}\left(\left(\dfrac{f}{400}\right)^{2}+1\right) + \left(18 + \dfrac{U}{10.28}\right) \\ \times\log_{10}\left(\dfrac{U}{4.63}\right), \quad (f \le 3200), \\ 50 - 10\cdot\log_{10}\left(\left(\dfrac{f}{3200}\right)^{2}+1\right) + \left(18 + \dfrac{U}{5.14}\right) \\ \times\log_{10}\left(\dfrac{U}{5.14}\right), \quad (6500 > f > 3200), \end{cases} \quad (5)$$

where f is frequency (Hz) and U is wind speed (m/s). Figure 4 shows the experimental noise spectrum levels and numerical results forecasted by the revised model for different wind speeds. The noise spectrum levels at the different wind speeds forecasted by the revised model are in good agreement with the experimental noise spectra. Due to the effects of shipping noise, the spectrum error at lower wind speeds (U<10 m/s) is about 2 dB at frequencies less than 800 Hz.

In summary, we conducted a wind-dominated ambient noise measurement experiment in the South China Sea to investigate the wind dependence of ambient noise in deep water. The selection of experiment data made it possible to accurately determine the relationship between the ocean ambient noise level and the wind speed. We observed an approximately quadratic noise-wind dependence in the frequency range of 0.5-3.2 kHz for local wind speeds exceeding 3 m/s. Based on this relationship, we obtained the ambient noise spectrum levels in the wind speed grouping. We developed a ray ambient noise model that uses a revised source level formula to predict the noise spectrum levels for different wind speeds. The good agreement between the wind-dominated ambient noise spectrum from the revised model and the experimental data confirms the validity of the model. This model can be used to predict wind-dependent ambient noise and to determine the relationship. In the future, we will use more experimental data to further validate this revised model.

This work was supported by the National Natural Science Foundation of China (Grant Nos. 11434012, 41561144006, and 11404366). We would like to express our great appreciation to all the staff for their help in the experiment, and we also thank TieJun Ling and XueMing Zhu for providing the meteorological data.

1 G. M. Wenz, J. Acoust. Soc. Am. **34**, 1936 (1962).
2 C. L. Piggott, J. Acoust. Soc. Am. **36**, 2152 (1964).
3 W. W. Crouch, and P. J. Burt, J. Acoust. Soc. Am. **51**, 1066 (1972).
4 Z. Klusek, and A. Lisimenka, J. Acoust. Soc. Am. **139**, 1537 (2016).
5 J. Y. Wang, and F. H. Li, Chin. Phys. B **25**, 124317 (2016).
6 S. Q. Liu, and F. H. Li, Sci. China-Phys. Mech. Astron. **46**, 094305 (2016).
7 H. T. Wen, Y. M. Yang, N. Wang, H. L. Ruan, and E. H. Huang, Chin. J. Acoust. **36**, 195 (2017).
8 R. M. Hamson, Appl. Acoust. **51**, 251 (1997).
9 H. Li, Z. L. Li, R. H. Zhang, and Z. H. Peng, Chin. Phys. Lett. **25**, 582 (2008).
10 J. H. Wilson, J. Acoust. Soc. Am. **73**, 211 (1983).
11 W. A. Kuperman, and M. C. Ferla, J. Acoust. Soc. Am. **77**, 2067 (1985).
12 D. J. Kewley, D. G. Browning, and W. M. Carey, J. Acoust. Soc. Am. **88**, 1894 (1990).
13 D. H. Cato, and S. Tavener, Appl. Acoust. **51**, 317 (1997).
14 D. M. Farmer, and D. D. Lemon, J. Phys. Oceanogr. **14**, 1762 (1984).
15 Z. L. Li, L. He, R. H. Zhang, F. H. Li, Y. X. Yu, and P. Lin, Sci. China-Phys. Mech. Astron. **58**, 014301 (2015).
16 C. H. Harrison, J. Acoust. Soc. Am. **99**, 2055 (1996).
17 Z. Li, and F. Li, Chin. J. Ocean. Limnol. **28**, 990 (2010).
18 C. H. Harrison, Appl. Acoust. **51**, 289 (1997).